

THE THREE-DIMENSIONAL STRUCTURES OF X-RAY BRIGHT POINTS

C. E. PARNELL, E. R. PRIEST

*Department of Mathematical and Computational Sciences, University of St. Andrews, Scotland,
KY16 9SS, U.K.*

and

L. GOLUB

Smithsonian Astrophysical Observatory, Cambridge, MA 02188, U.S.A.

(Received 19 October, 1993; in final form 26 January 1994)

Abstract. Recently, the Converging Flux Model has been proposed for X-ray bright points and cancelling magnetic features. The aim of this piece of work is to try and model theoretically specific X-ray bright points in the framework of the Converging Flux Model. The observational data used includes a magnetogram showing the normal component of the magnetic field at the photosphere and a high-resolution soft X-ray image from NIXT showing the brightenings in the lower solar corona. By approximating the flux concentrations in the magnetograms with poles of the appropriate sign and sense, the overlying three-dimensional potential field structure is calculated. Deduction of plausible motions of the flux sources are made which produce brightenings of the observed shape due to reconnection between neighbouring flux regions. Also the three-dimensional separatrix and separator structure and the way the magnetic field lines reconnect in three dimensions is deduced.

1. Introduction

X-ray bright points (BPs) were discovered by Vaiana *et al.* (1970) from X-ray images and their basic properties were studied by Golub *et al.* (1974, 1977); Golub, Krieger, and Vaiana (1976a, b) from *Skylab* images. They form in the corona as a diffuse cloud which grows at 1 km s^{-1} up to about 20 Mm followed by the appearance of a bright core of width 3 Mm which later fades as then does the diffuse cloud. The NIXT instrument (with much less scatter) has excellent spatial resolution and shows the true size of the BPs to be much smaller than the *Skylab* images (Priest, Parnell, and Martin, 1993) revealing them as beautiful and complex structures.

Opposite polarity photospheric magnetic fragments lie below the BP. A third of these magnetic fragments are believed to be *ephemeral active regions*, small areas of emerging magnetic flux; and two thirds are believed to be *cancelling magnetic features* (Martin, 1984), bipolar regions of magnetic flux which are approaching and cancelling.

An Emerging Flux Model by Heyvaerts, Priest, and Rust (1977), modeled analytically by Tur and Priest (1976) and numerically by Forbes and Priest (1984), explains how a BP might occur in terms of reconnection between newly emerging flux and an overlying field. In a recent paper, Priest, Parnell, and Martin (1993) put forward instead a Converging Flux Model for a BP and associated cancelling mag-

netic feature. In the Converging Flux Model two initially unconnected magnetic fragments are situated on the photosphere with an overlying background magnetic field. These magnetic fragments move towards each other and at a certain separation, the interactive distance, d , they form a null point at the photosphere. As the magnetic fragments continue moving together the null point rises to form an X-type neutral point reaching a maximum height, $\frac{1}{2}d$. Reconnection at the neutral point releases energy in the corona in the form of a BP and hot plasma is injected along the newly reconnected field lines. The neutral point then moves back down to the photosphere and, at zero separation of the magnetic fragments, photospheric reconnection gives rise to the associated cancelling magnetic feature often observed after the BP.

A theoretical study of two BPs (called *I* and *II*) observed by NIXT on 11 July, 1991 (eclipse day) has been carried out following along the lines of the Converging Flux Model. The observations are discussed in Section 2, and Section 3 outlines the stages involved in the study of each BP. Initially there is a consideration of the structure of the transverse magnetic field components in the photosphere. Then a purely two-dimensional (2D) look at all the poles lined up in the photosphere (along the x -axis) gives a simple view of the magnetic field line structure. Work in three-dimensions (3D) tries to model the magnetic structures emanating from the surface of the Sun, with emphasis on the form of the separatrix surfaces and the separator. Finally a comparison of the observed brightenings of the BP in the lower solar corona and possible reconnected (illuminated) field lines is made in an attempt to explain the structure of the BPs. In Section 4 bright point *I* is studied and Section 5 is the study of bright point *II*.

2. Observations

The BPs studied are from a full disc soft X-ray image (Figure 1) taken by the Normal Incident X-ray Telescope (NIXT) on a rocket flight on 11 July, 1991 at the same time as the eclipse totality seen from Hawaii. The NIXT instrument was launched on a NASA sounding rocket from White Sands Missile Range at 17:25 UT. NIXT observes the full disc of the Sun with a resolution less than $1''$; it is described in detail by Spiller *et al.* (1991). The multilayer mirror has a pass band of 1.4 \AA at 63.5 \AA and includes the wavelengths of the emission lines of Mg X and Fe XVI that are formed at temperatures $T \approx 10^6 \text{ K}$ and $3 \times 10^6 \text{ K}$, respectively.

The full disc X-ray image reveals five distinctive BPs, two of which are labelled *I* and *II* in Figure 1. This paper concentrates on BP's *I* and *II* which on enlarged X-ray images, Figure 2, are shown to have at least one brighter inner core, with a more diffuse cloud of complex structure extending outwards.

The corresponding Kitt Peak magnetograms taken on 11 July for the region directly below the BPs shows the normal component of the magnetic field. Contour plots made from the magnetograms, given at two resolutions (low resolution: Figures 3(a) and 3(b); high resolution: Figures 4 and 12), show the intensity and

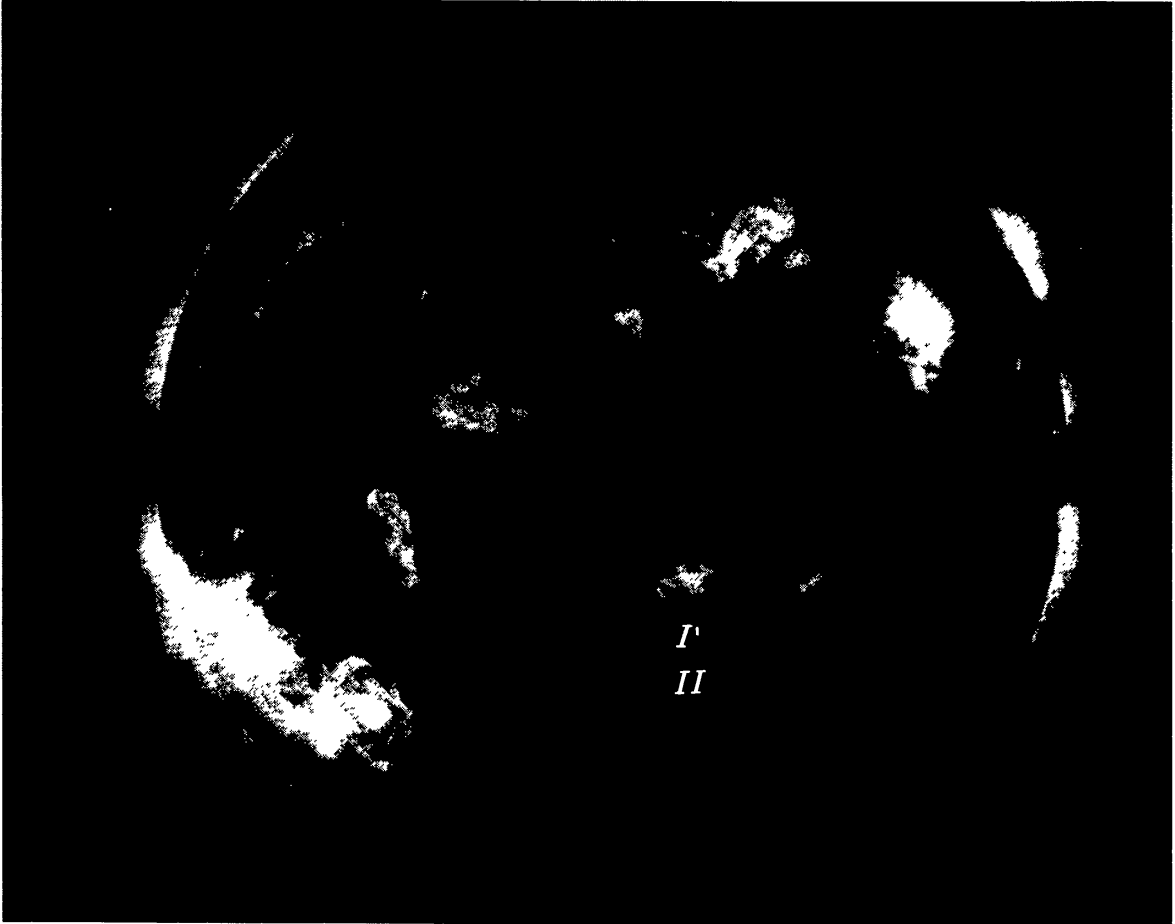


Fig. 1. A full-disc soft X-ray image of the Sun taken by the NIXT telescope on 11 July, 1991. The X-ray bright points studied are labelled *I* and *II*.

structure of the normal components of the magnetic field in the photosphere. The higher resolution contour plots have equivalent resolution to that of the NIXT full disc images. Regions of positive magnetic field are depicted by solid black contours and negative magnetic field regions by black dotted contours. The contour spacing varies from plot to plot (see figure captions), outlining positive and negative magnetic regions of various intensities and sizes. The following model tries to ascertain the most important features which give rise to the observed BP.

3. The Stages Involved in Each Bright Point Study

Initially the contour plots of the normal component of the magnetic field in conjunction with the soft X-ray image of the BP are considered and various questions asked. Which regions, positive or negative, are connected with the observed brightening? How are these regions likely to be moving, interacting, and evolving in order to cause the brightening?

Following the philosophy of the Converging Flux Model of Priest, Parnell, and

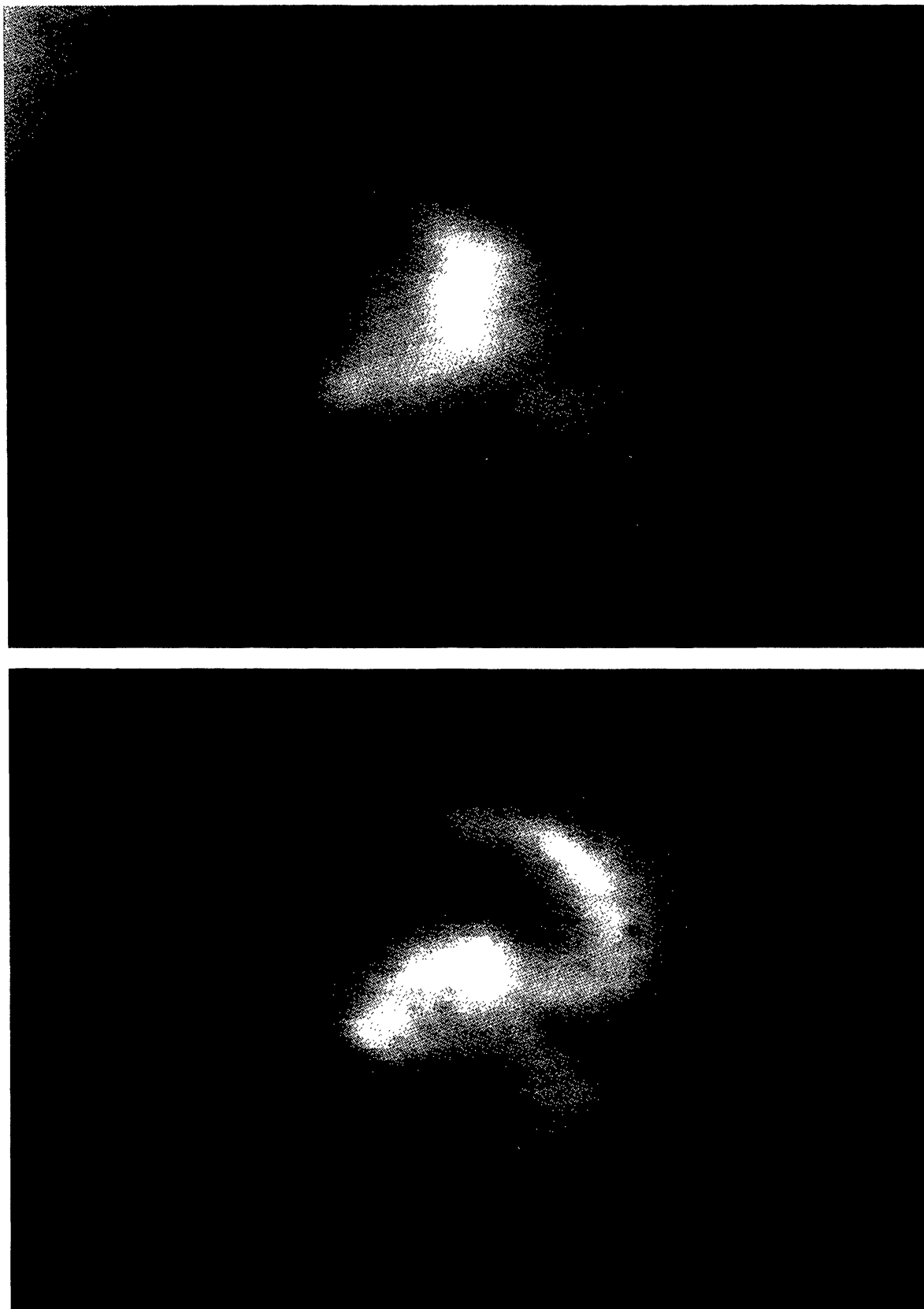


Fig. 2. The soft X-ray images of bright points *I* and *II* taken by the NIXT telescope on 11 July, 1991.

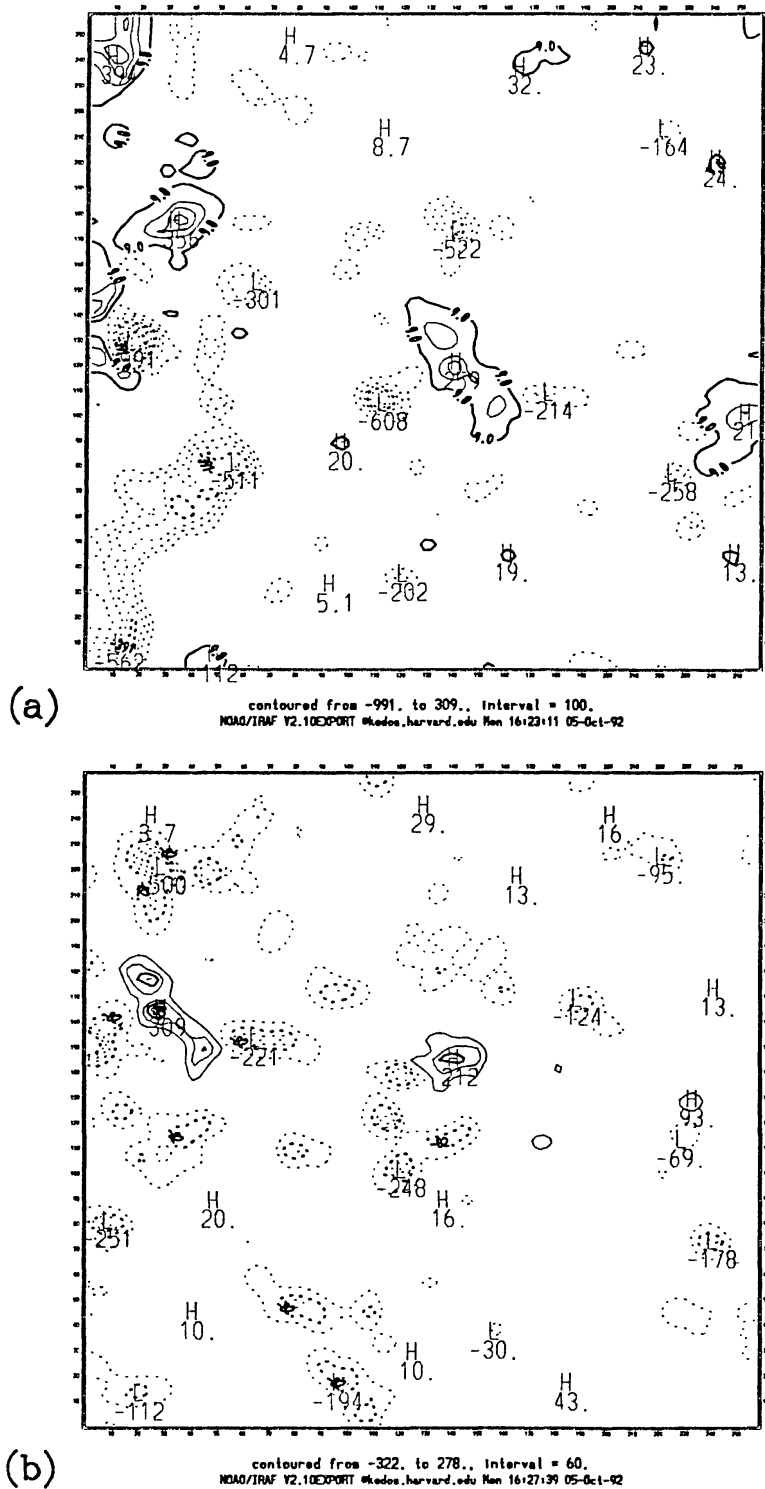


Fig. 3. The low-resolution contour plots taken from the Kitt Peak magnetogram corresponding to the area of the photosphere below bright points, (a) bright point *I* and (b) bright point *II*. Solid curves depict positive regions and dotted ones negative regions.

Martin (1993) a model for each specific BP can be set up consisting of poles of various strengths representing the magnetic regions believed to play vital roles in the life of the BP. According to this model, as these poles move, field lines

will reconnect and brighten due to the injection of heat or plasma along them by the reconnection process itself. Examples of this behaviour have been seen with *Yohkoh* (Tsuneta and Lemen, 1992; Shibata *et al.*, 1992; Strong *et al.*, 1992).

To model the magnetic fields it is assumed that there are no regions of emerging flux and that purely the movement and interaction (cancellation) of existing magnetic regions alone gives rise to the brightenings in the corona. Of course, due to the limited number of magnetograms available, the motion of these regions and the validity of this assumption are difficult to determine, but here it is taken as a working hypothesis. Possible motions of the important poles are considered and the final dynamic situation proposed for each BP because it is suggested by the Converging Flux Model and accounts for the observed brightenings in a natural way.

It is supposed that the photosphere below each BP consists of a series of discrete magnetic sources and sinks. Let Φ be the magnetic potential due to n poles, namely,

$$\Phi = \sum_{i=1}^n \frac{f_i}{((x - a_i)^2 + (y - b_i)^2 + z^2)^{1/2}}, \quad (3.1)$$

where f_i is strength of the pole i situated at position $(a_i, b_i, 0)$ on the photosphere ($z = 0$). Then the corresponding magnetic field ($\mathbf{B} = \nabla\Phi$) with components (B_x, B_y, B_z) is

$$\mathbf{B} = \left(\begin{aligned} &\sum_{i=1}^n \frac{-f_i(x - a_i)}{((x - a_i)^2 + (y - b_i)^2 + z^2)^{3/2}}, \\ &\sum_{i=1}^n \frac{-f_i(y - b_i)}{((x - a_i)^2 + (y - b_i)^2 + z^2)^{3/2}}, \\ &\sum_{i=1}^n \frac{-f_i z}{((x - a_i)^2 + (y - b_i)^2 + z^2)^{3/2}} \end{aligned} \right). \quad (3.2)$$

In both cases two plots of the magnetic field lines transverse to the photosphere are drawn. These show the *separatrices*, the surfaces field lines which divide topologically distinct regions and extend to or from the X-type neutral points, the reconnection points in the photosphere. In the first plot the magnetic poles are in the positions dictated by the observed magnetic contour plots for the given BP and in the second plot one magnetic pole is moved. A comparison of these two plots enables a decision to be made as to which field lines are likely to have been reconnected and which field lines would therefore brighten.

A schematic 2D depiction of the reconnection in each BP may be set up by placing poles in a straight line and considering the resulting magnetic field above the photosphere. Using complex variable theory let $z = x + iy$, where the z -axis is the line in the photosphere along which the poles lie and the y -axis is directed

vertically upwards from the photosphere. Define a complex magnetic potential \mathcal{B} , as $\mathcal{B}(z) = B_y + iB_x$, where $\mathbf{B}(x, y) = B_x\hat{e}_x + B_y\hat{e}_y$, so that

$$\mathcal{B}(z) = \sum_{i=1}^n \frac{f_i}{(z - a_i)}, \quad (3.3)$$

where n is the number of poles and f_i is the strength of pole i situated at position $(a_i, 0)$ on the photosphere. This has a corresponding flux function \mathcal{A} satisfying $\mathbf{B} = \nabla \times \mathbf{A}$, where $\mathbf{A} = \mathcal{A}\hat{e}_z$. Therefore, $B_x = \partial\mathcal{A}/\partial y$, $B_y = -\partial\mathcal{A}/\partial x$ and

$$\mathcal{A}(x, y) = \sum_{i=1}^n f_i \text{Arg} \left(\frac{a_i - z}{a_i} \right). \quad (3.4)$$

In 3D, using the form for the magnetic field given in Equation (3.2), the separatrix surfaces and the separator may be drawn. *Separatrix surfaces* are the 3D extension of 2D separatrices and divide topologically distinct regions. The *separator* is the intersection of the separatrix surfaces, it is a field line that extends from one neutral point to another. When a pole is moved, field lines near the separator reconnect to form new field lines which brighten due to the injection of heat and plasma along them. Now if it is assumed that coronal cooling is dominated by conduction and if the constant pressure form for the energy equation with energy losses due to conductivity only is considered, it has the form

$$\rho c_p \frac{DT}{Dt} = -\nabla \cdot \mathbf{q}, \quad (3.5)$$

where c_p is the specific heat at a constant pressure, and \mathbf{q} is the heat flux function which can be written as

$$\mathbf{q} = -\kappa \nabla T, \quad (3.6)$$

where κ is the thermal conduction tensor. Conduction parallel to the field lines is much greater than conduction perpendicular, so κ is assumed to be κ_{\parallel} . By performing a dimensional analysis Equation (3.5) determines the conduction time as

$$\tau_{\text{cond}} = \frac{\rho c_p L^2}{\kappa_{\parallel}}. \quad (3.7)$$

The typical coronal value of κ_{\parallel} is approximately $9 \times 10^{-12} T^{5/2} \text{ W m}^{-1} \text{ K}^{-1}$, the temperature T is $\sim 2 \times 10^6 \text{ K}$, and the density ρ is $8.36 \times 10^{-13} \text{ kg m}^{-3}$. If the length of the loop L is taken as $5 \times 10^7 \text{ m}$ ($\approx 50 \text{ Mm}$), then $\tau_{\text{cond}} \approx 850 \text{ s}$.

The typical velocity of a field line in the corona is between 1 and 10 km s^{-1} and therefore, taking the average velocity as 5 km s^{-1} , the distance, d_{bri} , a field line may move whilst bright, before cooling, is

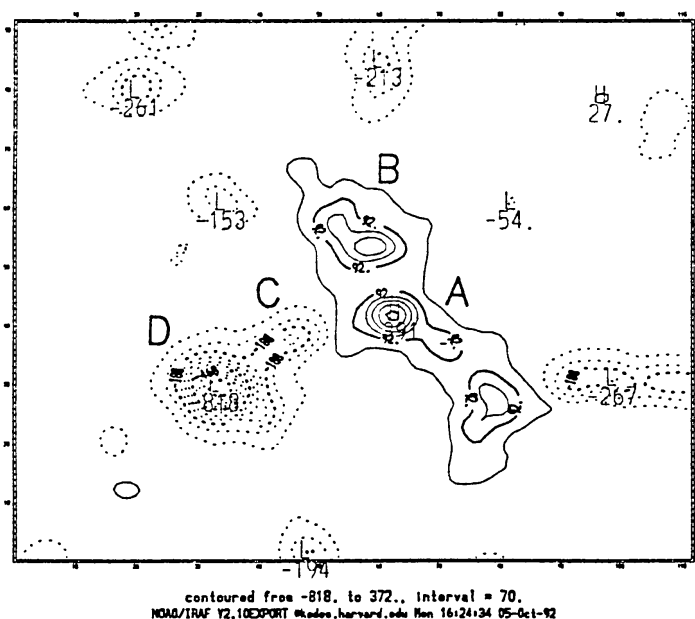


Fig. 4. Bright point *I*'s high-resolution contour plot taken from the Kitt Peak magnetogram. Solid curves depict positive regions and dotted ones negative regions. The main magnetic regions *A*, *B*, *C*, and *D* believed to be involved in the formation of the bright point are labeled.

$$d_{br i} = 5 \times 10^3 \times 850 = 4.3 \times 10^6 \text{ m (4 Mm)}. \quad (3.8)$$

So the reconnection and movement of the 'bright' field lines may be fast relative to the time it takes for the hot plasma along the field lines to cool. This means that a large number of field lines could be bright at any one time.

4. Bright Point *I*

In the specific case of bright point *I* it is supposed that the photosphere below the BP consists of four main magnetic regions *A*, *B*, *C*, and *D* labeled in Figure 4. Poles *A*, *B*, *C*, and *D* are estimated to have strengths 2.9, 1.7, -1.3 , and -16.6 ($\times 10^{19}$ Mx) and to be situated in positions (1.0, 0.0, 0.0), (0.87, 0.69, 0.0), (0.0, 0.0, 0.0), and $(-0.76, -0.33, 0.0)$, respectively. The origin is taken as the centre of magnetic region *C*, the small negative region, and the direction of a line from pole *C* to pole *A* is taken to be along the *x*-axis. A distance of one unit corresponds to approximately 10 Mm (14 arc sec) on the Sun.

By using Equation (3.4) a plot of the magnetic field lines transverse to the photosphere can be drawn (Figure 5(a)). It is assumed that pole *C* is moving towards pole *B* and away from poles *A* and *D* to position (0.5, 0.4, 0.0), as shown in Figure 5(b). As pole *C* moves, field lines from *A* to *C* and from *B* to *D* will reconnect to form new field lines from *A* to *D* and from *B* to *C*. Heat or plasma injected along these lines causes them to brighten. The brighter inner core is thought to be situated in the lower solar corona over the neutral points, the centres of reconnection in the photosphere, as sketched in Figure 6.

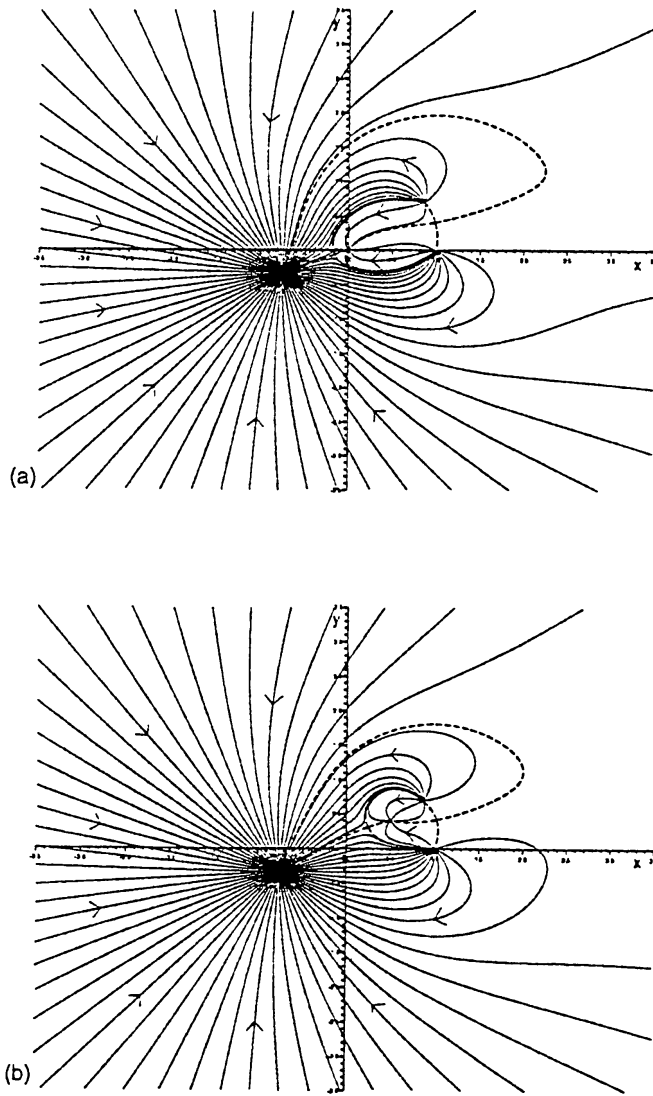


Fig. 5. (a) A contour plot for bright point *I* of the potential magnetic field lines lying in the photosphere, due to poles of strengths 2.9, 1.7, -1.3 , and -16.6 , respectively, positioned at *A* (1.0, 0.0), *B* (0.87, 0.69), *C* (0.0, 0.0), and *D* (-0.76 , -0.33) in the $z = 0$ plane. (b) Corresponding potential field lines when the pole *C* of strength -1.3 has moved to (0.5, 0.4) in the $z = 0$ plane.

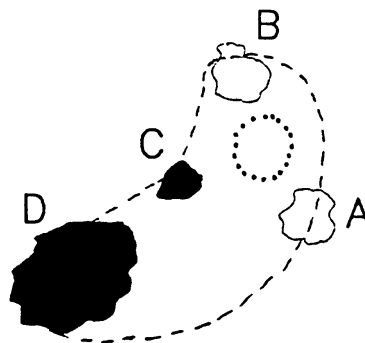


Fig. 6. A sketch of the relative position of bright point *I*, outlined by the dashed line, with the brighter inner core, outlined by the dotted line, above the positive magnetic poles *A* and *B* (shaded in white), and the negative magnetic poles *C* and *D* (shaded in black) in the photosphere.

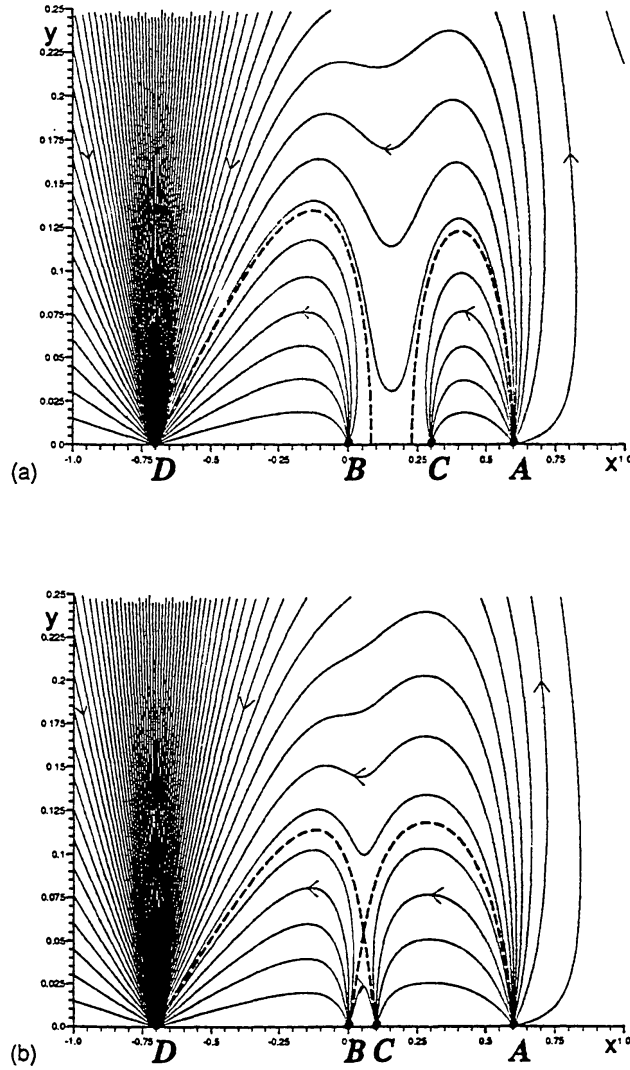


Fig. 7. (a) Magnetic field lines due to poles of strengths 2.9, 1.7, -1.3 , -16.6 and at positions 0.6, 0.0, 0.3, and -0.7 , respectively, along the x -axis. (b) Corresponding field lines when the pole of strength -1.3 has moved from 0.3 to 0.1 on the x -axis.

The schematic 2D depiction of the reconnection is set up by situating poles A , B , C , and D of strengths 2.9, 1.7, -1.3 , and -16.6 at 0.6, 0.0, 0.3, and -0.7 , respectively on the x -axis (Figure 7(a)). Pole C of strength -1.3 moves to 0.1 on the x -axis as shown in Figure 7(b), with new field lines from B to C and from A to D being formed and illuminated.

Using the strengths and initial positions relating to the 2D transverse magnetic field line plots for this BP, the separatrix surfaces and the separator are drawn (Figure 8). Figures 9(a) and 9(b) show the separator and the structure of the magnetic field lines lying in each of these surfaces. It is interesting to note that the large separatrix surface is made up of field lines starting from the far neutral point and ending at either of the two negative poles and that the smaller separatrix surface is made up of fieldlines starting from either of the two positive poles and ending at the near neutral point. The separator is the only field line that starts at the

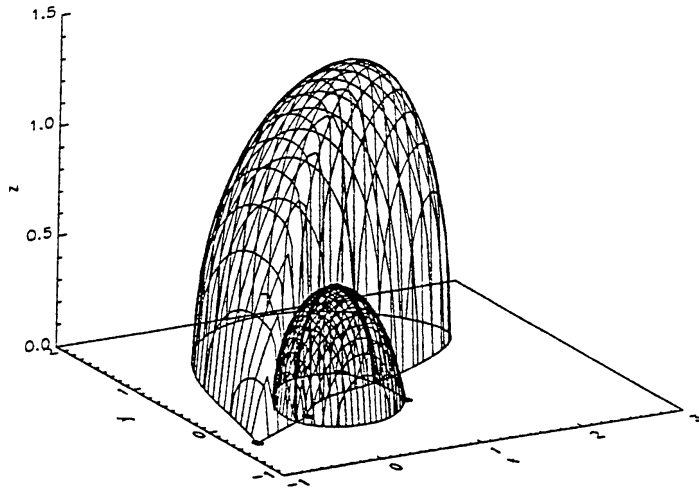


Fig. 8. The shape of the separatrix surfaces and the separator (thick) is shown due to poles (labeled by dots) of strengths 2.9, 1.7, -1.3 , -16.6 at positions A (1.0, 0.0), B (0.87, 0.69), C (0.0, 0.0), and D (-0.76 , -0.33), respectively, in the $z = 0$ plane.

far neutral point and ends at the near one. Figure 10(a) shows two field lines lying in different topological regions near the separator, one magnetic field line going from pole A to pole C and the other from pole B to pole D . The effect of pole C (strength -1.3 and position (0.0, 0.0, 0.0)) moving nearer pole B (strength 1.7 and position (0.87, 0.69, 0.0)) is to cause the field lines from A to C and from B to D near the separator to reconnect and form field lines from B to C and from A to D (Figures 10(b)). These new field lines will brighten due to the injection of heat and plasma along them. The reconnection and movement of the 'bright' field lines may be fast relative to the time it takes for the hot plasma along the field lines to cool. This would mean the field lines shown in Figure 11(a) would be bright. Looking down from above, these field lines outline a similar shape to that seen in the soft X-ray image of BP I . If instead pole C was assumed to be moving away from pole B and towards pole A , it would cause field lines from B to C and A to D to reconnect to give lines from A to C and from B to D . These would brighten as shown in Figure 11(b). The resulting brightening would not correspond to that in the soft X-ray image of BP I , since the resulting bright field lines would outline a different shape from that seen in the soft X-ray image.

5. Bright Point II

The photosphere below bright point II is assumed to consist of four main magnetic regions A , B , C , and D labelled in Figure 12. The strengths 6.6, -0.9 , -1.1 , -1.4 ($\times 10^{19}$ Mx) and positions (0.0, 0.0, 0.0), (-0.33 , 1.46, 0.0), (0.0, -1.39 , 0.0), and (-0.93 , -0.33 , 0.0) correspond respectively to the poles A , B , C , and D . Pole A , the only positive pole, is taken to lie at the origin with the negative y -axis in the direction of a line from pole A to pole C . As before a distance of one unit

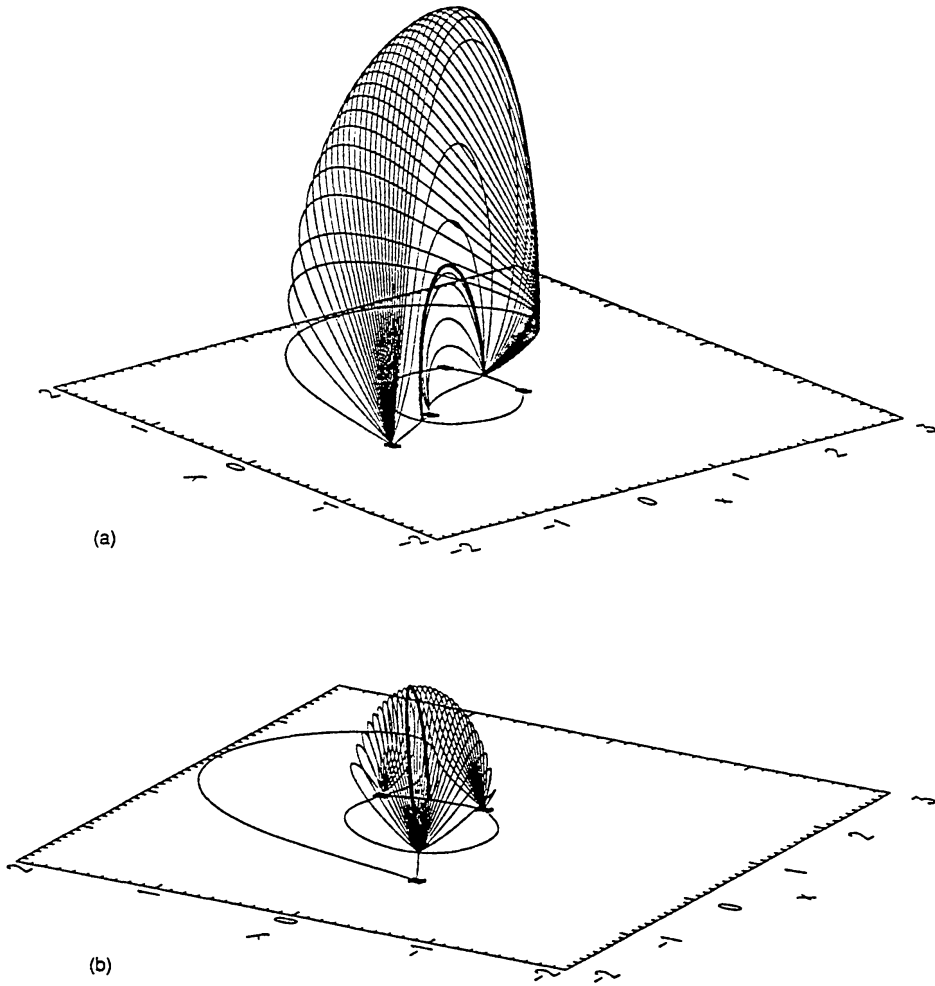


Fig. 9. The structure of the magnetic field lines lying in the separatrix surfaces and passing through (a) the negative poles and (b) the positive poles of bright point I .

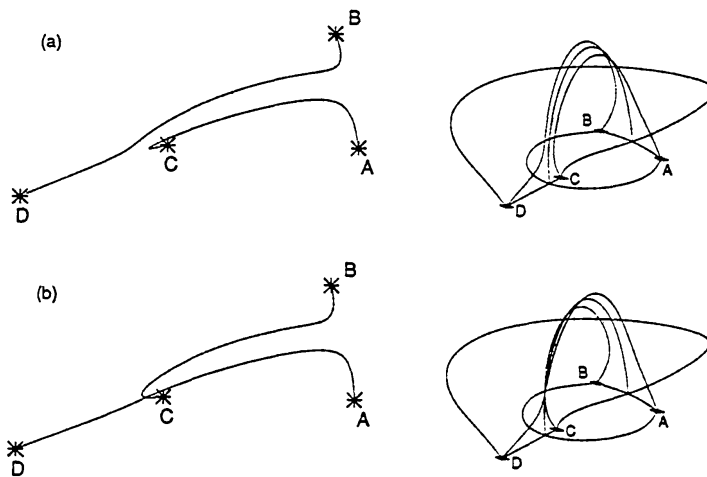


Fig. 10. Bright point I . (a) Two initial magnetic field lines, one from pole A to C and one from pole B to D lying in topologically distinct regions near the separator viewed from above and from the side. (b) Two corresponding reconnected magnetic field lines, one from pole A to D and the other from pole B to C .

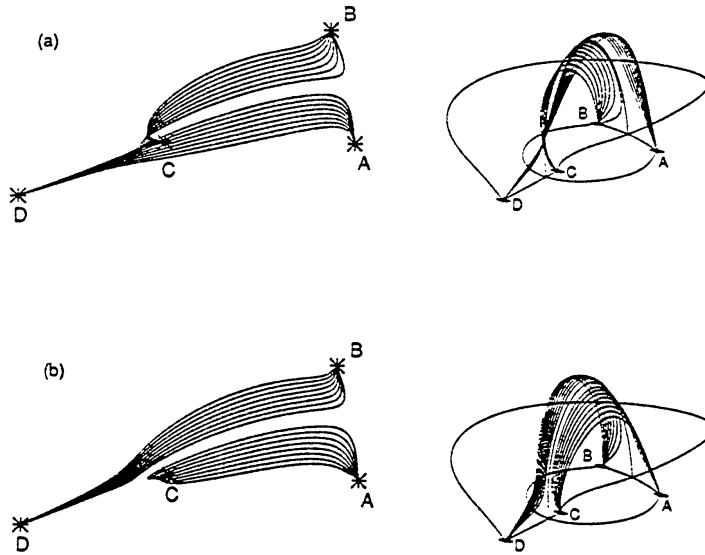


Fig. 11. Bright point *I*. (a) Several magnetic field lines, from poles *A* to *D* and *B* to *C* which have been reconnected due to the movement of pole *C* towards pole *B* and away from pole *A*, viewed from above and from the side. (b) Several reconnected magnetic field lines, from poles *A* to *C* and *B* to *D* which have been reconnected due to the movement of pole *C* towards pole *A* and away from pole *B*.

corresponds to approximately 10 Mm (14 arc sec) on the Sun.

The transverse magnetic fields are plotted in Figure 13(a). In Figure 13(b) it is assumed that pole *A* has moved towards pole *D*, way from poles *B* and *C* to position $(-0.4, -0.2, 0.0)$ causing field lines originally unconnected to either *B*, *C*, or *D*, and lying in between poles *B* and *C* to reconnect; either they can reconnect with field lines from *A* to *B* to form new lines from *A* to *B* and from *A* extending outwards, unconnected to *B*, *C*, or *D* and lying between *B* and *D*; or they can reconnect with field lines from *A* to *C* to form new field lines from *A* extending outwards lying between *C* and *D* that are unconnected to *B*, *C*, or *D* and new field lines from *A* to *C*. The movement also causes field lines originally unconnected to either *B*, *C*, or *D* and lying between poles *D* and *B* to reconnect with lines from *A* to *D* to form new field lines from *A* to *D* and field lines extending outwards from *A* lying between *D* and *C* but unconnected to either pole. The newly reconnected field lines, injected with plasma or heat are believed to brighten. New field lines from *A* to *B*, *A* to *C*, and *A* to *D* brighten, but the new field lines from *A* extending outwards, unconnected to either *B*, *C*, or *D* do not brighten. This may be because the heat along these very long field lines spreads out or the plasma injected is spread along the length of the field lines so that it is not visible in soft X-rays. The three bright cores of BP *II* overlie the centres of reconnection at the X-type neutral points and the positive pole *A*. Since the upper arm of the BP is more distinctive than the lower it is likely that more field lines from *A* to *B* are reconnected than from *A* to *C* as would be produced by a movement down and across of the positive pole *A*. (See Figure 14.)

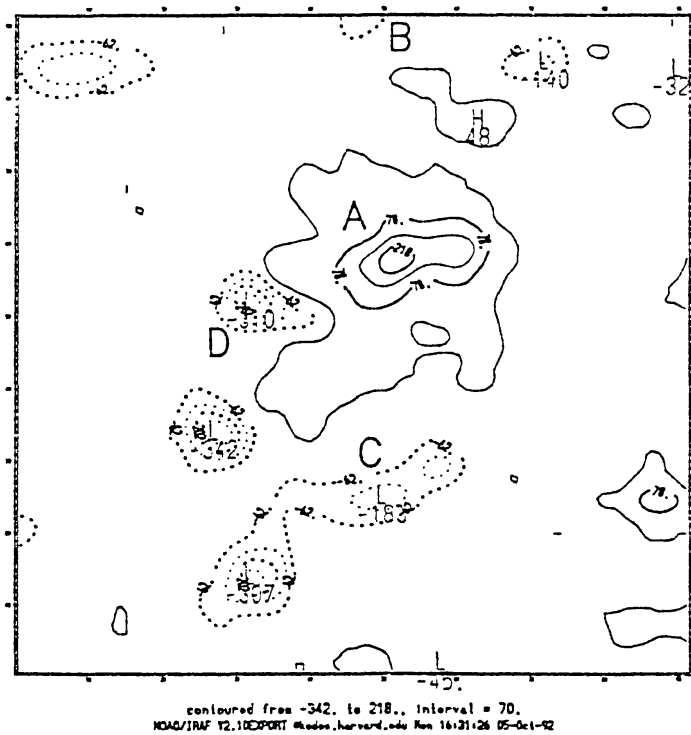


Fig. 12. A high-resolution contour plot taken from the Kitt Peak magnetogram of the photosphere below bright point *II*. Solid curves depict positive regions and dotted ones negative regions. The main magnetic regions *A*, *B*, *C*, and *D* believed to be involved in the formation of the bright point are labeled.

In this case the 2D side-on view used to give a simplified look at the reconnection is set up by poles *A*, *B* (or *C*), and *D* of strengths 6.6, -0.9 , and -1.4 being placed at 0.0, 0.6, and -0.5 , respectively, on the x -axis (Figure 15(a)). Figure 15(b) has pole *A* of strength 6.6 situated at -0.25 on the x -axis as shown. These figures do not indicate that any reconnection has taken place as pole *A* has moved, so the reconnection can only be seen, in this case, by looking at the field lines in the $z = 0$ plane or in 3D.

In 3D, as for BP *I*, the strengths and initial positions relating to the poles in the 2D transverse magnetic field plots for this BP are used, and again using Equation (3.2) the separatrix surfaces are drawn. There are six separatrix surfaces (Figure 16). Three have a dome shape, as seen in Figure 8 for BP *I*, and enclose field lines from the positive pole to just one of the poles *B*, *C*, or *D*. The three other separatrix surfaces, are vertical planes which divide field lines extending out from the two sides of a dome. The domes are constructed of field lines in the surface from positive pole *A* to a neutral point lying in the photosphere. The vertical planes intersect the photosphere along the field line from the three-dimensional neutral point to either the negative pole enclosed in the dome or extending outwards to a distant negative pole. Figure 17 shows the newly reconnected field lines believed to remain bright when the positive pole *A* moves near pole *D*. As in the discussion

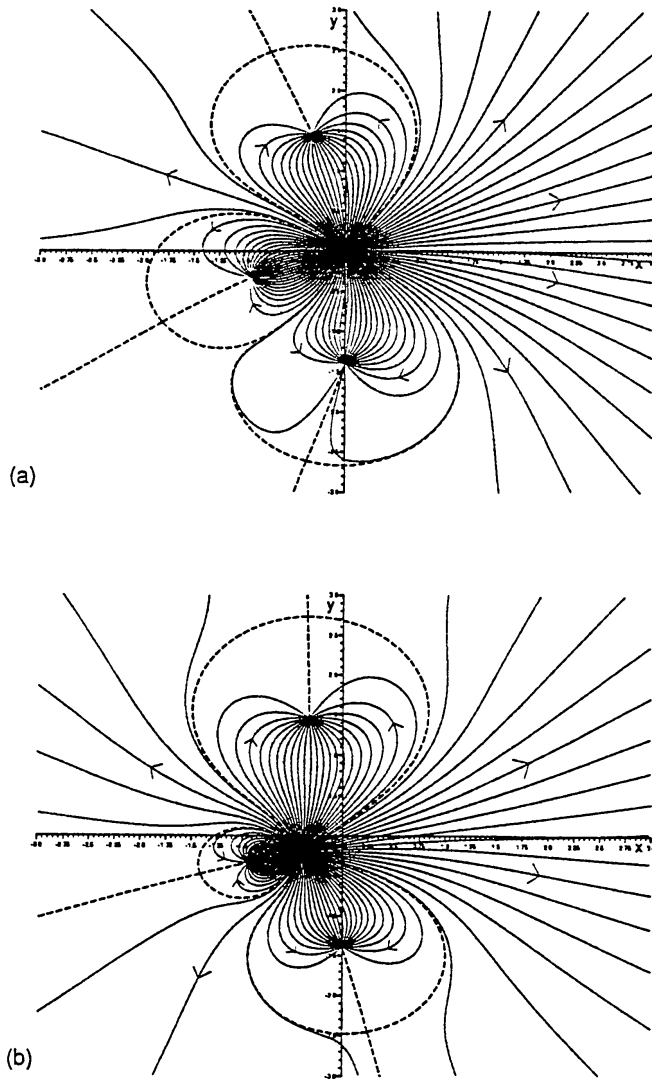


Fig. 13. (a) A contour plot of the photospheric potential magnetic field lines related to bright point *II*, with poles of strengths 6.6, -0.9 , -1.1 , and -1.4 , respectively, positioned at *A* (0.0, 0.0), *B* (-0.33 , 1.46), *C* (0.0, -1.39), and *D* (-0.93 , -0.33) in $z = 0$ plane. (b) Corresponding potential field lines when the pole *A* of strength 6.6 has moved to (-0.4 , -0.2) in the $z = 0$ plane.

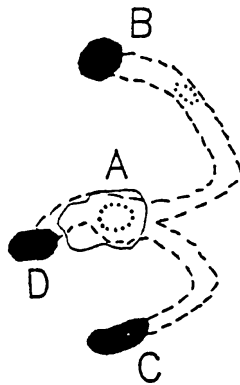


Fig. 14. A sketch of the relative positions of bright point *II*, outlined by the dashed curves and its brighter inner cores, outlined by the dotted curves, above the positive magnetic pole *A* (shaded in white), and the negative magnetic poles *B*, *C*, and *D* (shaded in black) in the photosphere.

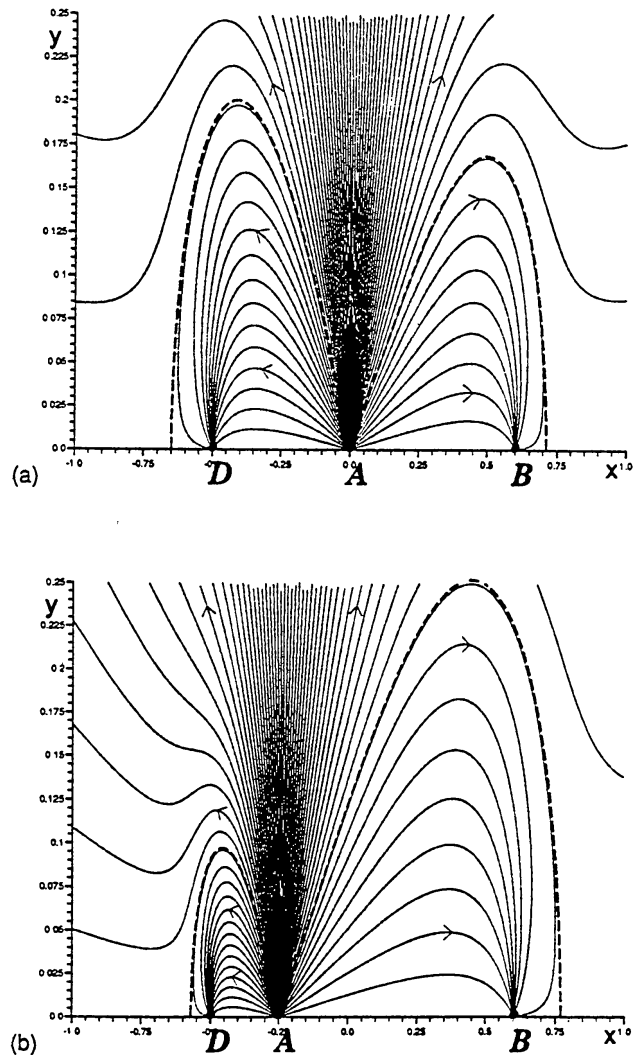


Fig. 15. (a) Magnetic field lines due to poles of strengths 6.6, -0.9 , -1.4 and at positions A 0.0, B 0.6, D -0.5 , respectively, along the x -axis. (b) Corresponding field lines when the pole of strength 6.63 is moved from 0.0 to -0.25 along the x -axis in the photosphere below bright point II .

for the transverse field plot it is assumed that the long unconnected field lines will not brighten and that the reconnection and motion of the bright field lines is faster than the cooling time of the hot plasma along the field lines.

6. Conclusion

By the use of Priest, Parnell, and Martin's (1993) Converging Flux Model for X-ray bright points, we have been able to develop a plausible explanation for the observed brightenings from the high-resolution soft X-ray image of BPs I and II . It was assumed that only the movement and interaction of magnetic regions caused the BPs. As the magnetic regions move together, reconnection takes place at the three-dimensional neutral points and along the separator to form newly reconnected field lines which are injected with heat or plasma and brighten in the shape of the observed form.

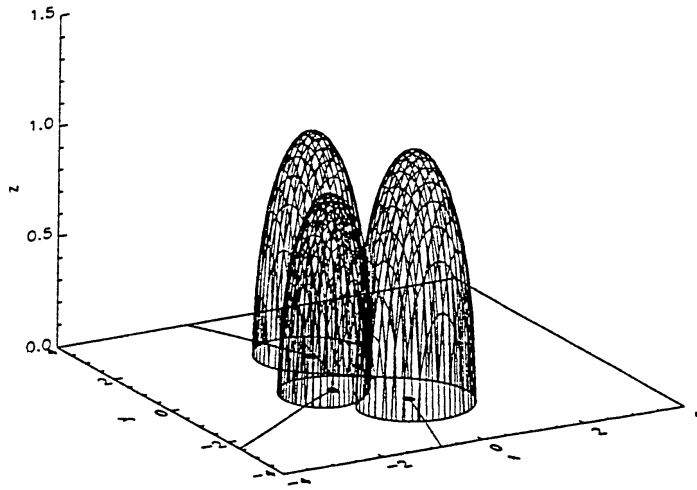


Fig. 16. The shape of the separatrix surfaces of bright point *II*, due to poles (labeled by dots) of strengths 6.6, -0.9 , -1.1 , -1.4 at positions *A* (0.0, 0.0), *B* (-0.33 , 1.46), *C* (0.0, -1.39), and *D* (-0.93 , -0.33), respectively, in the $z = 0$ plane.

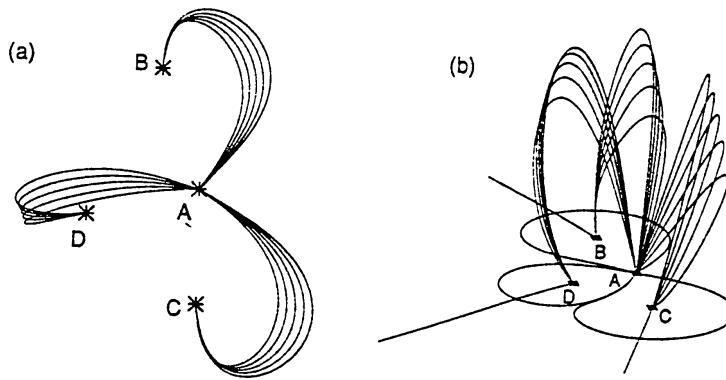


Fig. 17. Several reconnected field lines from pole *A* to *B*, *A* to *C*, and *A* to *D* which are believed to brighten and cause the observed soft X-ray image for bright point *II*.

Contour plots from Kitt Peak magnetograms of the photosphere below the BP were studied and the magnetic regions believed to play key roles were modeled as point sources and point sinks. It is suspected in both cases that four magnetic regions (two positive and two negative for BP *I*, and one positive and three negative for BP *II*), are central to the formation and life of the BPs. Field lines from these magnetic poles are sketched in 2D and 3D just before and after reconnection. By assuming the movement of a particular pole it was found that the field lines injected with heat or plasma (and therefore bright) were approximately the shape and size of the observed soft X-ray brightenings for the BP and the brighter inner cores overlie the centres of reconnection on the separator, so being heated directly from the reconnection itself.

In this study the behaviour predicted is of a natural and simple nature, relying on the motion of the magnetic regions and cancellation of flux to release energy to create the BP. This is likely not always to be the case, since emergence of flux

can also cause BPs, but in general many more BPs are likely to be created by cancellation than emergence (Priest, Parnell, and Martin, 1993). The importance of these two effects is likely to vary from one BP to another (Webb *et al.*, 1993; Harvey, 1985). The limited number of high-resolution observations of BPs means there is no firm evidence as to what direction the different poles are moving or whether there is any important flux emergence, but models have been set up here which do lead to a reasonable explanation for the BPs. It stresses the importance of having in the future coordinated observations at high resolution in both space and time from magnetograms, $H\alpha$ and soft X-rays.

Acknowledgements

C. E. Parnell and E. R. Priest are delighted to acknowledge the UK Science and Engineering Research Council for their financial support. We are also most grateful to the SPARCS team at White Sands Missile Range for making the launch of the NIXT instrument possible. L. Golub was supported by NASA under Grant NAG5-626. Thanks also to S. McClymont (via G. Rickard) for the three-dimensional graphics.

References

- Forbes, T. G. and Priest, E. R.: 1984, *Solar Phys.* **94**, 315.
 Golub, L., Krieger, A. S., and Vaiana, G. S.: 1976a, *Solar Phys.* **49**, 79.
 Golub, L., Krieger, A. S., and Vaiana, G. S.: 1976b, *Solar Phys.* **50**, 311.
 Golub, L., Krieger, A. S., Silk, J., Timothy, A. and Vaiana, G.: 1974, *Astrophys. J.* **189**, L93.
 Golub, L., Krieger, A. S., Harvey, J., and Vaiana, G.: 1977, *Solar Phys.* **53**, 111.
 Harvey, K. L.: 1985, *Australian J. Phys.* **38**, 875.
 Heyvaerts, J., Priest, E. R., and Rust, D. M.: 1977, *Astrophys. J.* **216**, 123.
 Martin, S. F.: 1984, in S. Keil (ed.), *Small-Scale Dynamical Processes in Stellar Atmospheres*, Sacramento Peak Observatory, p. 30.
 Martin, S. F., Livi, S. H. B., Wang, J., and Shi, Z.: 1984, in M. Hagyard (ed.), *Measurements of Solar Vector Magnetic Fields*, NASA CP 2374, p. 403.
 Priest, E. R., Parnell, C. E., and Martin, S. F.: 1993, *Astrophys. J.*, submitted.
 Schmieder, B., Golub, L., and Antiochos, S. K.: 1993, preprint.
 Shibata, K., Nozawa, S., and Matsumoto, R.: 1992, *Publ. Astron. Soc. Japan* **44**, 265.
 Shibata, K., Ishido, Y., Acton, L., Strong, K., Hirayama, T., Uchida, Y., McAllister, A., Matsumoto, R., Tsuneta, S., Shimizu, T., Hara, H., Sakurai, T., Ichimoto, K., Nishino, Y., and Ogawara, K.: 1992, *Publ. Astron. Soc. Japan* **44**, L173.
 Spiller, E., McCorkle, R. A., Wilczynski, J. S., Golub, L., Nystrom, G., Takacs, P. Z., and Welch, C.: 1991, *Opt. Engn.* **30**, 1109.
 Strong, K., Harvey, K., Hirayama, T., Nitta, N., Schimizu, T., and Tsuneta, S.: 1992, *Publ. Astron. Soc. Japan* **44**, L161.
 Tsuneta, S. and Lemen, J. R.: 1992, in J. K. Linsky and S. Serio (eds.), *Physics of Solar and Stellar Coronae*, p. 113.
 Tur, T. J. and Priest E. R.: 1976, *Solar Phys.* **48**, 89.
 Vaiana, G. S., Krieger, A. S., Van Speybroeck, L. P., and Zehnpfennig, T.: 1970, *Bull. Am. Phys. Soc.* **15**, 611.
 Webb, D. F., Martin, S. F., Moses, D., and Harvey, J. W.: 1993, *Solar Phys.* **144**, 15.